Silica hollow-core anti-resonant fiber for harsh environment mid-infrared sensing applications

Xavier Insou, Simon Le Méhauté, Loïc Bodiou, Sébastien Claudot, Laurent Provino, Adil Haboucha, David Landais, Achille Monteville, Olivier Le Goffic, Thierry Taunay, et al.

Silica hollow-core anti-resonant fiber for harsh environment mid infrared sensing applications

Xavier Insou[a,b], Simon Le Méhauté[a], Loïc Bodiou[a], Sebastien Claudot[b], Laurent Provino[c], Adil Haboucha[c], David Landais[c], Achille Monteville[c], Olivier Le Goffic[c], Thierry Taunay[c,*], David Méchin[c], Lionel Quétel[d], Thierry Chartier[a], Joël Charrier[a], and Monique Thual[a]

[a]Univ Rennes, CNRS, Institut FOTON - UMR 6082, F-22305 Lannion, France
[b]SOURIAU, ITD, Eaton, 89 Route de Saint-Hubert, 72470 Champagné, France
[c]Photonics Bretagne, 4 Louis de Broglie, 22300 Lannion, France
[d]IDIL Fibres Optiques, Espace Corinne Erhel, 4 Rue Louis de Broglie, 22300 Lannion, France
[*]*currently* at Lumibird, 2 Rue Paul Sabatier, 22300 Lannion, France

ABSTRACT

Mid-infrared absorption spectroscopy is nowadays considered as a routine analysis and sensing tool providing highly discriminatory information on organic and inorganic molecules. The specific needs of the transport, aerospace or energy industries may involve applications for which the spectroscopic sensor has to withstand high temperatures. This paper reports the design and fabrication of a silica hollow-core anti-resonant fiber with 8 non-touching capillaries primarily designed for mid-infrared CO_x sensing inside engines. Numerical and analytical simulations performed to ensure fiber transparency in the 4-5 µm region are reported. Optical transmission between $3.9\,\mu m$ and $4.7\,\mu m$ is observed and demonstrate attenuation below $1\,dB/m$ for single capillary ring fibers in this range. A preliminary scheme for CO_2 sensing using a quantum cascade laser operating in one of the fiber's transmission windows ($\lambda = 4.3\ \mu m$) is depicted.

Keywords: fiber optics, mid infrared, hollow-core, gas sensing, combustion

1. INTRODUCTION

Laser absorption spectroscopy (LAS) is a widespread technique for selective and sensitive chemical species detection.[1,2] This technique can be used for a lot of practical applications,[3] both in the atmosphere or some specific space. The mid-infrared (Mid-IR) spectral range ($\sim 3 - 20\ \mu m$) is of high interest because almost all target molecules for environmental monitoring,[4] chemical warfare agents and explosives detection,[5] leak detection[6] or medical diagnosis[7] exhibit fundamentals rovibrational absorption bands in this region. Those fundamental vibrations are usually one to three orders of magnitude stronger than the so-called *overtones* or *combination bands* occurring in near-infrared (NIR) region. The recent progress in both Mid-IR laser (quantum cascade laser, optical parametric oscillators and Mid-IR fiber lasers) and photo-detector technologies has facilitated the development of active sensors in that spectral range.

For the transport, energy and aerospace industries in particular, carbon oxides and nitrogen oxides (CO_x, NO_x) are important target molecules in order to characterize combustion processes. The determination of thermodynamics and chemical properties of combustion gases in reactive flow can help mastering engines efficiency and prevent premature aging. To limit the impact of emissions on the environment and human health, a quantification of combustion products is required. Mid-IR and NIR LAS sensors able to assess chemical and thermodynamics information in reactive flows have established themselves as useful remote sensing tools regarding this type of applications.[8,9]

This study consists of the development of LAS and fiber-based sensors in the Mid-IR region for harsh environments applications as depicted in Figure 1. Firstly, the sensor consists of a modulated Mid-IR emitter

---

Further author information: (Send correspondence to Loïc Bodiou)
E-mail: loic.bodiou@univ-rennes1.fr, Telephone: +33 (0)2 96 46 93 72

(typically a quantum cascade laser or QCL) in order to perform LAS measurements. Active optical systems for spectroscopic measurement often rely on optical fibers to convey (and/or collect) the optical signal towards (from) the specific space of interest. By design, optical fibers (specially silica fibers) make the sensor mostly alignment and vibrations-free, compact and thus suited for on-the-field applications. Ideally, the chosen optical fiber link would be simultaneously able to withstand high temperatures and convey Mid-IR radiation to a centimetric length probe with insert(s) located directly in the gas flow. The signal will be collected and returned to the photodetector by means of a similar fiber link. The primary target application of the project would be in-flight monitoring of combustion gases in commercial aircraft turbines.
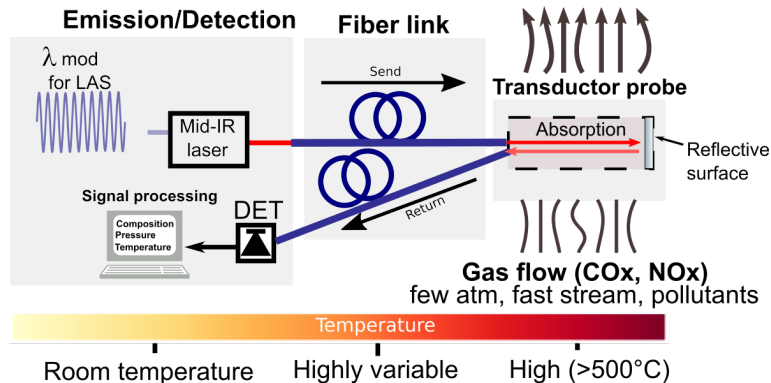

Figure 1. Targeted architecture for the development of fibered Mid-IR sensors dedicated to combustion gases characterization

This target application involves high temperatures, pressure, speed and pollution from engines exhaust gases. For sensors operating in the Mid-IR region, commons types of non-oxide fibers (namely chalcogenides, fluorides) can efficiently transmit these range of wavelength. Fiber-based Mid-IR CO_2 sensing has already been demonstrated in the literature.[10] However, non-oxide fibers are not necessarily compatible with high-temperatures applications without active cooling.[11] On the contrary, a hollow-core anti-resonant fiber[12] (HC-ARF) made of silica glass has lower temperature sensitivity and can thus operate up to $1000°C$.[13] Such thermal behaviour would allow to maintain the sensor integrity in high and fluctuating temperature environments (such as commercial planes engines), making of HC-ARF an interesting transmission channel for spectroscopic probing in harsh environments. The present paper will focus on the fabrication, design and characterization of a HC-ARF (Section 2) as an optical link for CO_x sensing and lay the foundations of a practical CO_2 LAS sensing method (Section 3) using quantum cascade laser (QCL) emitting around a 4.3 μm.

2. A HOLLOW-CORE ANTI-RESONANT FIBER

2.1 Interest of a vacuum guide

The confinement of light in air by the mean of micro-structured optical fibers has been of high interest since the first experimental demonstration twenty years from now.[14] Such a "vacuum guide" is generally referred as hollow-core fiber[15] (HCF). As opposed to traditional solid-core, step-index fibers where the guiding principle is total internal reflection, HCF either rely on photonic crystals[16] or anti-resonant core wall (*e.g.* tubes elements) for the structure to exhibit the desired waveguide behaviour. Fibers integrating these micro-structured cladding, and the respective refractive index modulations, have unique optical properties, notably the ability for guided modes to display losses lower than the bulk material. This opens-up the possibilities to transmit Mid-IR radiation inside a structure made of SiO_2, despite its virtually null optical transmission for wavelength longer than 3.6 μm.[17] Propagation losses of $50\,dB/m$ had been shown up to 8 μm whereas losses in solid-core silica fibers exceeds $10^6\,dB/m$ in this region[18] .

Because light mostly travels inside the air core, the advantages of HCF are indeed numerous. It allows a reduced latency of $\sim 30\%$ in comparison of solid-core glass fibers. Such an effect is of course highly desirable for

time-sensitive optical communications.[19] As light-matter interaction is weaker, optical damage and non-linear thresholds are increased while Fresnel reflections and losses are minimized. The last argument also makes HCF highly suitable for high-peak power applications in both NIR and Mid-IR.[20] On the contrary, one can purposely fill HCF with fluids (either liquid or gas) to enhance non-linearities of laser-fluid interaction thus optimizing high harmonics generation[21] or obtain laser operation relying on stimulated Raman scattering.[22,23] As for molecular spectroscopy, a low volume of the gas of interest can also be inserted in the HCF, thus maximizing path length without the need of sometimes bulky and unstable multi-pass cells. Trace gas sensors with detection limits at ppm or ppb levels were recently implemented using gas-filled HC-ARF for CO_x and NO_x[24-28] As for anti-resonant silica-air structures in particular, a design composed of a single ring of several capillaries (as seen of Figure 2b) has emerged over the year. This design is also referred as negative curvature[12] or "revolver" fibers.[29] In these structures, the significant reduction of overlap between the guided mode and the silica capillaries enables low fiber attenuation in the Mid-IR.

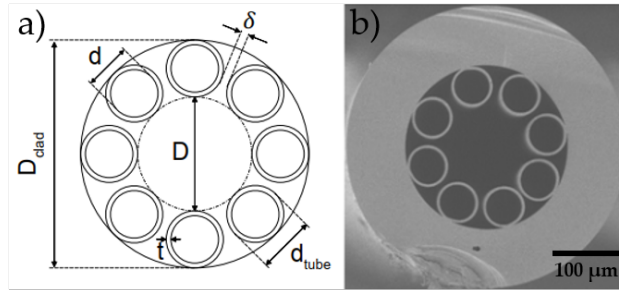## 2.2 Design, fabrication and experimental characterization of a HC-ARF

Figure 2. Structure of the detailed HC-ARF (a) sketch of the geometrical specifications, here $d = 52.7\,\mu m$, $D = 118.5\,\mu m$, $t = 3.6\,\mu m$, $\delta = 8.4\,\mu m$ (b) as viewed under electron microscope

A silica hollow-core fiber with 8 non-touching capillaries has been fabricated through a process similar to stack-and-draw technique. The fiber is described by its geometrical parameters, namely the core diameter D as well as the diameter d, thickness t and spacing δ of the tubes (Figure 2a). The resulting structure is shown under microscope in Figure 2b. The parameters D, d, t and δ obviously influence the propagation properties, respectively the propagation losses, the singlemode/multimode behaviour of the waveguide, the position of the transmissions bands and the confinement efficiency.

2.2.1 Transmission spectral range and confinement losses

Guidance in HC-ARFs is due to reflections in the capillaries walls that act as Fabry-Perot cavity, thus preventing particular wavelengths from being confined (hence the *antiresonant* or *inhibited coupling* designations). The theoretical spectral transmission bands and confinement losses, mostly influenced by parameters D and t, has been calculated using Bache et. al's analytical model,[30] considering the geometrical parameters specified in the legend of figure 2. The result is displayed on Figure 3 (solid black curve). The dashed grey curve shows the same calculation for $t = 3\,\mu m$ (instead of $3.6\,\mu m$) to illustrate the influence of the capillaries wall thickness. The results are plotted together with the absorption-cross section of commons combustion products (CO_x, NO_x and water vapor) in the Mid-IR region (color curves). The molecular absorption cross-sections were calculated at 500K and 2 atm to match the expected measurement conditions of the aircraft engine exhaust gases. One can observe a good overlap between low fiber attenuation and strong CO_x absorption lines in so called "Band 2". Taking advantage of high purity silicate-based glasses thermo-mechanical, chemical resistance and low attenuation, the designed fiber could enable the development of a simultaneous CO and CO_2 spectroscopic Mid-IR sensor suited for harsh environments.
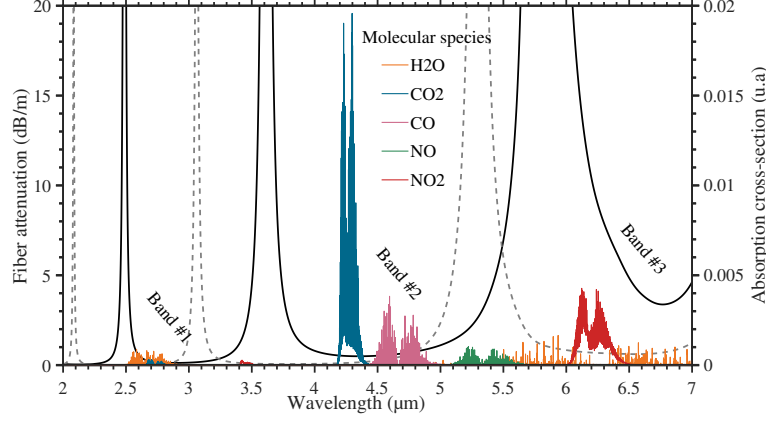
Figure 3. Analytical simulations of transmission bands of an HC-ARF for different capillary wall thicknesses t = 3 µm (dashed grey curve) and t = 3.6 µm (solid black curve). Mid-IR absorption bands of several gases (color curves) are also displayed. Molar absorption cross-section was calculated at 500K and 2 atm. The spectroscopic calculation has been made with HITRAN2020 database[31] and the transmission band calculation is based on Bache et al.[30]

2.2.2 HC-ARF attenuation

Thanks to the simple analytical simulation presented above, the fiber was designed to have a low attenuation around 4.4 µm where strong CO_x absorption lines lies. To obtain more realistic attenuation values, a full vectorial approach (FEM, Comsol Multiphysics) was also used. These calculations were performed between 3.6 µm and 4.7 µm and yield an estimation of the mode field diameter of 91 µm at 4 µm and losses values displayed in Figure 4.
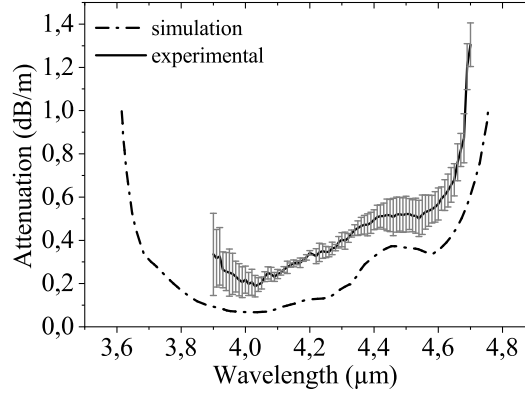

Figure 4. Fiber attenuation between 3.7 and 4.9 μm. The dashed curve is a numerical calculation (finite-element) of the fundamental mode losses. The solid curve and grey points present the experimental result and error obtained from the cut-back method, carried out for three HC-ARF lengths between 3 and 24 m

Experimental measurements were also carried out with a Daylight Solutions MIRCAT-QT QCL operating between 3.9 and 4.7 μm. The propagation losses coefficient has been measured with the traditional "cut-back" method using 24, 21 and 3 meters of fibers in both directions. In addition, the fiber was purged for the duration of the measurements, to avoid strong CO_2 absorption. Experimental results and associated errors are presented in Figure 4. A slightly multi-mode behaviour could explain the offset between theory and measurement despite a good overall agreement. Nevertheless, the measurements shows an attenuation well below $1 dB/m$ for most of the transmission band, and the lowest measured attenuation 0.19 dB/m is recorded at 4.03 µm. Low attenuation of 0.35 dB/m and 0.54 dB/m were measured respectively at 4.26 µm and 4.58 µm, which corresponds to the wavelengths of maximum absorption from carbon oxides. These results demonstrate that the fabricated fiber

displays propagation loss values comparable or lower than those reported in the literature (compiled in Table 1 below).

Authors	Year	Core diameter D	Wall thickness t	Losses	λ
CO_2 sensing around 4.2 µm					
Kolyadin et al.[18]	2013	119 µm	6 µm	4 dB/m	4.1 µm
Yu et al.[32]	2013	n.d	n.d	0.15 dB/m	4.2 µm
Pryamikov et al.[33]	2011	68 µm	n.d	2 dB/m	4.25 µm
Present work	2022	118 µm	3.6 µm	**0.35 dB/m**	**4.26 µm**
CO sensing around 4.5 µm					
Gladyshev et al.[34]	2017	77 µm	1.15 µm	0.92 dB/m	4.4 µm
Yu et al.[32]	2013	n.d	n.d	0.47 dB/m	4.4 µm
Astapovich et al.[35]	2019	75 µm	n.d	1.1 dB/m	4.42 µm
Nikodem et al.[26]	2019	62 µm	1.6 µm	6 dB/m	4.54 µm
Present work	2022	118 µm	3.6 µm	**0.54 dB/m**	**4.58 µm**

Table 1. Fiber losses in the 4-5 µm region for similar revolver designs in the literature. (n.d = not discussed)

3. MID-IR GAS SENSING METHODOLOGY

3.1 Setup and measurement principle

In parallel of the design and fabrication of the previously detailed HC-ARF, a sensing method has been investigated for CO_2. The goal is to determine the target gas concentration by measuring its absorbance using laser absorption spectroscopy. Assuming the target gas is the only absorbing species in the mixture, the absorbance is simply defined by Beer-Lambert law (Eq.1). It consists of the product of absorption-cross section ε ($molec^{-1}.cm^3.m^{-1}$), the target gas concentration c ($molec.cm^{-3}$) and the interaction length l. In practice, the absorbance is computed as the logarithm of the laser intensity is presence of the absorbing species (I_T) and a reference laser intensity (I_0).

$$A(\lambda) = \varepsilon(\lambda)cl = -ln(I_T(\lambda)/I_0(\lambda)) \tag{1}$$

The Direct Absorption Spectroscopy[2] (DAS) is the most straightforward version of laser absorption spectroscopy due to limited equipment required for its implementation, quick alignment and interpretation of raw data. In practice, such method may be sufficient because carbon dioxide displays strong absorbance in the 4.3 μm range, even over short interaction lengths (*i.e. cm* scale). DAS consists of a simple slow-frequency (few Hz) spectral sweep around a chosen absorption line of the target gas as depicted in Figure 5. After measurement of the transmitted intensity $I_T(\lambda)$, the baseline $I_0(\lambda)$ is usually assessed with a polynomial fit performed off-resonance.[26] The computed absorbance is then fitted (least-square) with a numerical absorbance model in order to estimate the chemical composition X and/or pressure P and temperature T.

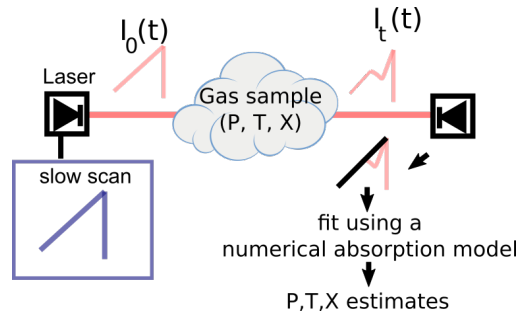Figure 5. General principle of Direct Absorption Spectroscopy (DAS)

The particular DAS setup used in this study consists of a frequency swept ($f = 100\,Hz$) quantum cascade laser (QCL) operating near strong CO_2 resonances around 4.3 μm, an 10 cm open gas cell with CaF_2 windows filled with a mixture of diluted CO_2 in N_2 (whose concentration can be tuned using mass flow controllers) and a $HgCdTe$ (MCT) photodetector. An optical chopper is also used to extinguish the laser signal periodically, synchronized with the sweep frequency, in order to asses and remove the influence of the photo-detector dark current.

3.2 Line choice and wavelength evolution

The evolution of the emitted wavelength with the operating temperature of the laser and applied voltage had been characterized with a HORIBA iHR320 grating spectrometer in a static (*i.e.* non modulated) configuration. The result is shown in Figure 6a. The modulation voltage dependency shows a non-negligible second order contribution. By changing its operating temperature, the QCL can reach several absorption lines of CO_2, including four "major" and three "minor" lines (Figure 6b). Even for atmospheric level (around 500 parts per million), the transmission is found to be below 30% over $l = 10$ cm if the QCL operates at a "major" line. For this reason, the spectral scan has been set around a "minor" line ($\lambda = 4299.23 \pm 0.2nm$) to obtain a wider dynamic range relative to the sensor noise floor.
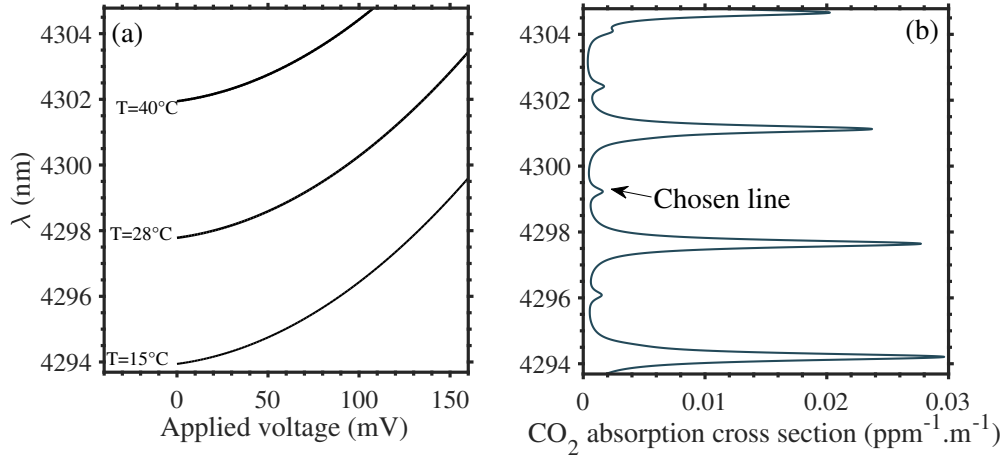

Figure 6. Wavelength dependency of (a) the QCL laser signal with respect to temperature and applied modulation voltage (b) CO_2 absorption cross-section in the same region

3.3 Measured absorbance and concentration estimation

An experiment with increasing CO_2 concentration inside the cell was performed. The absorbance is computed as the ratio of the transmitted laser intensities (I_T) and baseline I_0 (linear fit at the extremities of the spectral scan). A least-square estimation is then performed using the following absorbance model :

$$A(c, \Delta, \lambda) = \varepsilon(\lambda, T, P)cl + \Delta \tag{2}$$

Here, the free parameters are the concentration c (here in $\%\,vol$) and an offset Δ which is due to the lack of non-absorbing wings inside the spectral sweep (*i.e* no true zero absorbance points). The fitting method considers $T = 296\,K, P = 1\,atm$, both air and self-broadening contribution of the absorption linewidth. No significant error due to temperature and pressure is expected as the cell remained opened during the experiment. However, one can expect a potential bias on the estimated concentration due to baseline estimation, an asymmetric absorption line and offset compensation Δ. Even if this bias is expected to be below 10 % by processing simulated signals, these effects have to be further investigated. As for now, the measured (and offset corrected) absorbance and corresponding fits for several CO_2 dilutions are displayed Figure 7a with respect to the wavenumber ν (inverse wavelength expressed in cm^{-1}). One notes the expected increase of the absorbance by up to two orders

of magnitude with increasing CO_2 concentration. Absorption in a saturation regime can even be observed (blue curve) where the transmitted optical power reaches the photo-detection noise floor (around $C = 1.8\%\,vol$ according to the least-square fit of the absorbance). Despite an expected bias on the side of the absorption line, the resulting fits are satisfying at the absorption peak (Figure 7b).
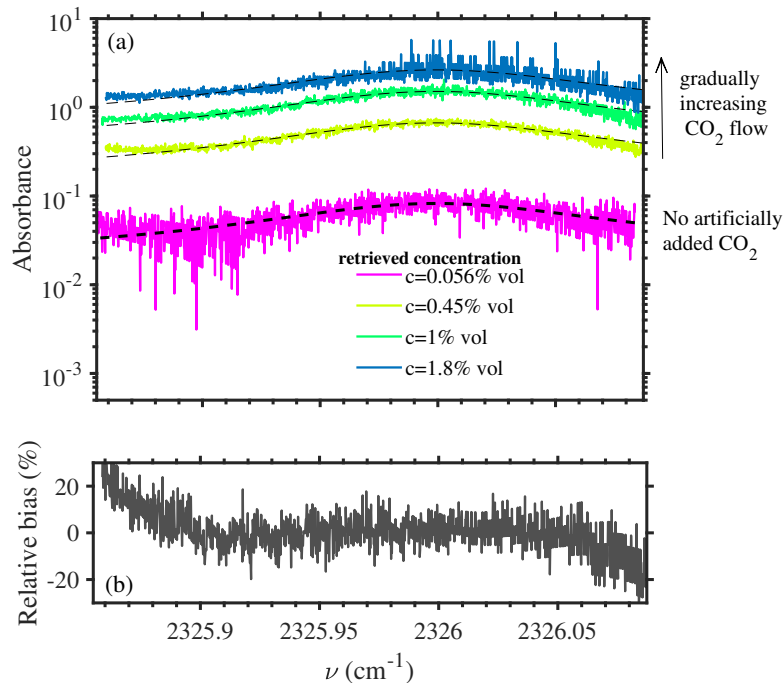

Figure 7. (a) Computed and offset corrected absorbance and fits for an empty-cell and several CO_2 dilutions in N_2 (b) typical relative bias between fits and experimental absorbance

The present results had not been correlated with another sensor as for now. However, the retrieved mixing ratio with no artificially added CO_2 (purple curve) inside the cell is $0.56\,\%\,vol$. This result constitutes a first calibration in itself because it is close to the expected atmospheric CO_2 level (as verified with a tabletop gas sensor). The evolution of the retrieved concentration (from 0.56 to $1.8\,\%\,vol$) with an increasing carbon dioxide flow clearly demonstrates the setup sensitivity to the target gas. This result also shows the sensitivity procured by the DAS technique could be sufficient for CO_2 measurement in the few % vol range over centimetric interaction length.

4. CONCLUSION

The design of a low mid-IR attenuation silica HC-ARF was reported. Numerical simulations were performed to design a HC-ARF transparent in the 4-5 µm region. The fiber was fabricated and then characterized in terms of transmission over the 3.9-4.7 µm wavelength range. Attenuation down to 0.35 dB/m and 0.54 dB/m propagation losses are measured for wavelengths equal to λ=4.26 µm and λ=4.58 µm, corresponding, respectively, to the wavelengths of maximum absorption from CO_2 and CO gases. These results could pave the way to the implementation of this kind of fiber as a hybrid transmission link in mid-IR spectroscopic systems, validating at the same time the use of numerical simulation to design a specific fiber for mid-IR in-situ gas monitoring. Direct absorption measurements of CO_2 with a modulated QCL operating at the transmission band of the HC-ARF had been carried out. Additional environmental tests such as temperature and vibration and bending sensitivity should also be performed in order to better assess the fiber behaviour in harsh environments.

ACKNOWLEDGMENTS

REFERENCES

[1] Li, J., Yu, Z., Du, Z., Ji, Y., and Liu, C., "Standoff chemical detection using laser absorption spectroscopy: a review," *Remote Sensing* **12**(17), 2771 (2020).

[2] Wang, Z., Fu, P., and Chao, X., "Laser absorption sensing systems: Challenges, modeling, and design optimization," *Applied Sciences* **9**, 2723 (jul 2019).

[3] Tittel, F. K., Richter, D., and Fried, A., "Mid-infrared laser applications in spectroscopy," *Solid-state mid-infrared laser sources* , 458–529 (2003).

[4] Nelson, D. D., McManus, B., Urbanski, S., Herndon, S., and Zahniser, M. S., "High precision measurements of atmospheric nitrous oxide and methane using thermoelectrically cooled mid-infrared quantum cascade lasers and detectors," *Spectrochimica Acta Part A: Molecular and Biomolecular Spectroscopy* **60**(14), 3325–3335 (2004).

[5] Bauer, C., Sharma, A., Willer, U., Burgmeier, J., Braunschweig, B., Schade, W., Blaser, S., Hvozdara, L., Müller, A., and Holl, G., "Potentials and limits of mid-infrared laser spectroscopy for the detection of explosives," *Applied Physics B* **92**(3), 327–333 (2008).

[6] Strahl, T., Herbst, J., Lambrecht, A., Maier, E., Steinebrunner, J., and Wöllenstein, J., "Methane leak detection by tunable laser spectroscopy and mid-infrared imaging," *Applied Optics* **60**(15), C68–C75 (2021).

[7] Henderson, B., Khodabakhsh, A., Metsälä, M., Ventrillard, I., Schmidt, F. M., Romanini, D., Ritchie, G. A., te Lintel Hekkert, S., Briot, R., Risby, T., et al., "Laser spectroscopy for breath analysis: towards clinical implementation," *Applied Physics B* **124**(8), 1–21 (2018).

[8] Goldenstein, C. S., Spearrin, R. M., Jeffries, J. B., and Hanson, R. K., "Infrared laser-absorption sensing for combustion gases," *Progress in Energy and Combustion Science* **60**, 132–176 (2017).

[9] Liu, C. and Xu, L., "Laser absorption spectroscopy for combustion diagnosis in reactive flows: A review," *Applied Spectroscopy Reviews* **54**(1), 1–44 (2019).

[10] Starecki, F., Charpentier, F., Doualan, J.-L., Quetel, L., Michel, K., Chahal, R., Troles, J., Bureau, B., Braud, A., Camy, P., et al., "Mid-ir optical sensor for co2 detection based on fluorescence absorbance of dy3+: Ga5ge20sb10s65 fibers," *Sensors and Actuators B: Chemical* **207**, 518–525 (2015).

[11] Artyushenko, V., Bocharnikov, A., Sakharova, T., and Usenov, I., "Mid-infrared fiber optics for 1—18 μm range: Ir-fibers and waveguides for laser power delivery and spectral sensing," *Optik & Photonik* **9**(4), 35–39 (2014).

[12] Yu, F. and Knight, J. C., "Negative curvature hollow-core optical fiber," *IEEE J. Sel. Top. Quantum Electron* **22**(2), 146–155 (2016).

[13] Liu, D., Wu, Q., Mei, C., Yuan, J., Xin, X., Mallik, A. K., Wei, F., Han, W., Kumar, R., Yu, C., et al., "Hollow core fiber based interferometer for high-temperature (1000° c) measurement," *Journal of Lightwave Technology* **36**(9), 1583–1590 (2018).

[14] Russell, P., "Photonic crystal fibers," *science* **299**(5605), 358–362 (2003).

[15] Belardi, W., "Hollow-core optical fibers," *Fibers* **7**(5), 50 (2019).

[16] Cregan, R., Mangan, B., Knight, J., Birks, T., Russell, P. S. J., Roberts, P., and Allan, D., "Single-mode photonic band gap guidance of light in air," *science* **285**(5433), 1537–1539 (1999).

[17] Pryamikov, A. D., Biriukov, A. S., Kosolapov, A. F., Plotnichenko, V. G., Semjonov, S. L., and Dianov, E. M., "Demonstration of a waveguide regime for a silica hollow-core microstructured optical fiber with a negative curvature of the core boundary in the spectral region¿ 3.5 μm," *Optics express* **19**(2), 1441–1448 (2011).

[18] Kolyadin, A. N., Kosolapov, A. F., Pryamikov, A. D., Biriukov, A. S., Plotnichenko, V. G., and Dianov, E. M., "Light transmission in negative curvature hollow core fiber in extremely high material loss region," *Optics express* **21**(8), 9514–9519 (2013).

[19] Zhu, B., Mangan, B. J., Kremp, T., Puc, G. S., Mikhailov, V., Dube, K., Dulashko, Y., Cortes, M., Marceau, K., Violette, B., et al., "First demonstration of hollow-core-fiber cable for low latency data transmission," in [*Optical Fiber Communication Conference*], Th4B–3, Optical Society of America (2020).

[20] Michieletto, M., Lyngsø, J. K., Jakobsen, C., Lægsgaard, J., Bang, O., and Alkeskjold, T. T., "Hollow-core fibers for high power pulse delivery," *Optics Express* **24**(7), 7103–7119 (2016).

[21] Heckl, O., Baer, C., Kränkel, C., Marchese, S., Schapper, F., Holler, M., Südmeyer, T., Robinson, J., Tisch, J., Couny, F., et al., "High harmonic generation in a gas-filled hollow-core photonic crystal fiber," *Applied Physics B* **97**(2), 369–373 (2009).

[22] Li, J., Li, H., and Wang, Z., "Application of hollow-core photonic crystal fibers in gas raman lasers operating at 1.7 μm," *Crystals* **11**(2), 121 (2021).

[23] Benabid, F., Knight, J. C., Antonopoulos, G., and Russell, P. S. J., "Stimulated raman scattering in hydrogen-filled hollow-core photonic crystal fiber," *Science* **298**(5592), 399–402 (2002).

[24] Nikodem, M., "Laser-based trace gas detection inside hollow-core fibers: A review," (sep 2020).

[25] Yao, C., Xiao, L., Gao, S., Wang, Y., Wang, P., Kan, R., Jin, W., and Ren, W., "Sub-ppm co detection in a sub-meter-long hollow-core negative curvature fiber using absorption spectroscopy at 2.3 μm," *Sensors and Actuators B: Chemical* **303**, 127238 (2020).

[26] Nikodem, M., Gomółka, G., Klimczak, M., Pysz, D., and Buczyński, R., "Demonstration of mid-infrared gas sensing using an anti-resonant hollow core fiber and a quantum cascade laser," **27**, 36350 (nov 2019).

[27] Jaworski, P., Kozioł, P., Krzempek, K., Wu, D., Yu, F., Bojeś, P., Dudzik, G., Liao, M., Abramski, K., and Knight, J., "Antiresonant hollow-core fiber-based dual gas sensor for detection of methane and carbon dioxide in the near-and mid-infrared regions," *Sensors* **20**(14), 3813 (2020).

[28] Krzempek, K., Jaworski, P., Kozioł, P., and Belardi, W., "Antiresonant hollow core fiber-assisted photothermal spectroscopy of nitric oxide at 5.26 μm with parts-per-billion sensitivity," *Sensors and Actuators B: Chemical* **345**, 130374 (2021).

[29] Bufetov, I. A., Kosolapov, A. F., Pryamikov, A. D., Gladyshev, A. V., Kolyadin, A. N., Krylov, A. A., Yatsenko, Y. P., and Biriukov, A. S., "Revolver hollow core optical fibers," *Fibers* **6**(2) (2018).

[30] Bache, M., Habib, M. S., Markos, C., and Lægsgaard, J., "Poor-man's model of hollow-core anti-resonant fibers," *JOSA B* **36**(1), 69–80 (2019).

[31] Gordon, I., Rothman, L., Hargreaves, R., Hashemi, R., Karlovets, E., Skinner, F., Conway, E., Hill, C., Kochanov, R., Tan, Y., et al., "The hitran2020 molecular spectroscopic database," *Journal of Quantitative Spectroscopy and Radiative Transfer* **277**, 107949 (2022).

[32] Yu, F. and Knight, J. C., "Spectral attenuation limits of silica hollow core negative curvature fiber," *Opt. Express* **21**, 21466–21471 (Sept. 2013).

[33] Pryamikov, A. D., Biriukov, A. S., Kosolapov, A. F., Plotnichenko, V. G., Semjonov, S. L., and Dianov, E. M., "Demonstration of a waveguide regime for a silica hollow - core microstructured optical fiber with a negative curvature of the core boundary in the spectral region ¿ 3.5 μm," *Opt. Express* **19**, 1441–1448 (Jan. 2011).

[34] Gladyshev, A. V., Kosolapov, A. F., Khudyakov, M. M., Yatsenko, Y. P., Kolyadin, A. N., Krylov, A. A., Pryamikov, A. D., Biriukov, A. S., Likhachev, M. E., Bufetov, I. A., and Dianov, E. M., "4.4 μm raman laser based on hollow-core silica fibre," *Quantum Electronics* **47**, 491–494 (May 2017).

[35] Astapovich, M. S., Gladyshev, A. V., Khudyakov, M. M., Kosolapov, A. F., Likhachev, M. E., and Bufetov, I. A., "Watt-level nanosecond 4.42-μm raman laser based on silica fiber," *IEEE Photonics Technology Letters* **31**(1), 78–81 (2018).